# Doping effects of Ru in $L_{0.5}Sr_{0.5}CoO_3$ ($L$=La, Pr, Nd, Sm, and Eu)

K. Yoshii[1,*] and H. Abe[2]
[1]*Japan Atomic Energy Research Institute, Mikazuki, Hyogo 679-5148, Japan*
[2]*National Institute for Materials Science, Tsukuba, Ibaraki 305-0047, Japan*
(Received 7 May 2002; revised manuscript received 27 August 2002; published 17 March 2003)

Structure, magnetism, and transport have been investigated for $L_{0.5}Sr_{0.5}Co_{1-x}Ru_xO_3$ ($L$=La, Pr, Nd, Sm, and Eu, $x$=0, 0.1, and 0.2), in which Ru is doped at the Co site in perovskites $L_{0.5}Sr_{0.5}CoO_3$. The structures of most of the compounds were refined to orthorhombic *Pnma*. The compounds $L_{0.5}Sr_{0.5}CoO_3$ ($x$=0) are metallic ferromagnets below Curie temperatures between ~250 and ~150 K. We found that Ru doping brings about the suppression of ferromagnetic order as well as the loss of metallicity. The Curie-Weiss analysis showed that the order (except for $L$=La) commonly changes into an antiferromagnetic type with the doping. For $L$=Sm and Eu with $x$=0.2, sharp cusps at around 50–60 K in the magnetization-temperature curves were ascribed to a spin-glass transition, a finding which was supported by measurements of ac magnetic susceptibility and magnetization relaxation. An origin of these phenomena is proposed by considering several factors such as the change of the spin states of Co induced by Ru doping.

DOI: 10.1103/PhysRevB.67.094408 PACS number(s): 75.50.Cc, 75.50.Lk, 72.20.−i, 71.27.+a

## I. INTRODUCTION

Recent studies have revealed peculiar magnetic and transport properties of perovskite cobalt oxides $L_{1-x}A_xCoO_3$ ($L$, lanthanides: $A$, alkaline-earth metals).[1–23] $LCoO_3$ ($x$=0) containing only $Co^{3+}$ ($3d^6$) is an insulating material showing no magnetic order. Substitution of the $A^{2+}$ ions gives rise to a partial oxidation of $Co^{3+}$ into $Co^{4+}$ ($3d^5$) and results in ferromagnetic order with Curie temperatures ($T_C$) lower than ~280 K. Their properties have been most intensively studied for $La_{1-x}Sr_xCoO_3$ (Refs. 1–8), in which the six spin states of Co are possible: low-spin state (LS state: $t_{2g}^6e_g^0$ for $Co^{3+}$, $t_{2g}^5e_g^0$ for $Co^{4+}$), intermediate-spin state (IS state: $t_{2g}^5e_g^1$ for $Co^{3+}$, $t_{2g}^4e_g^1$ for $Co^{4+}$), and high-spin state (HS state: $t_{2g}^4e_g^2$ for $Co^{3+}$, $t_{2g}^3e_g^2$ for $Co^{4+}$). Complex changes in the magnetic behavior against $x$ have been interpreted as is described in the following.[1,3] In a very low Sr substitution ($x<\sim0.1$), each $Co^{4+}$ ion is preferably surrounded by six $Co^{3+}$ ions. The intermediate spin state of $t_g^5e_g^{(1-x)}$ is formed among the Co ions. These $Co^{3+}$ and $Co^{4+}$ ions are ferromagnetically coupled due to an electron transfer between the $e_g$ orbitals. Small Co clusters exhibit superparamagnetic behavior. The size of each cluster becomes larger for $\sim0.1\leqslant x\leqslant\sim0.18$. Antiferromagnetic interactions between the clusters lead to spin-glass phenomena. In the larger-$x$ region, the clusters become large enough to change the system into a metallic ferromagnet showing cluster-glass behavior. In this region, the ferromagnetism is assumed to be of an itinerant electron type.

This mechanism is very analogous to that for perovskite manganites $L_{1-x}A_xMnO_3$.[24] $LMnO_3$ ($x$=0) containing only $Mn^{3+}$ ($3d^4$,$t_{2g}^3e_g^1$) is an antiferromagnetic insulator. With the substitution of the $A^{2+}$ ions for $L^{3+}$, ferromagnetic order is observed with $T_C$ below ~400 K due to the ferromagnetic interaction between $Mn^{3+}$ ($t_{2g}^3e_g^1$) and $Mn^{4+}$ ($t_{2g}^3e_g^0$) through an electron transfer between the $e_g$ orbitals, called the double-exchange interaction. The discovery of the colossal magnetoresistance in these compounds has stimulated considerable renewed attention to their magnetic and electronic properties. Recently, the effects of Ru doping at the Mn site in $Sm_{1-y}Ca_yMnO_3$ were investigated.[24] The results showed that expansion of ferromagnetism and metallicity occurs in a wide composition region. This phenomenon was much more pronounced than in Cr doping. These results were explained in connection with several factors, such as orbital reorientation and ferromagnetic interactions between Mn and Ru.

In this work, structure, magnetism, and transport have been investigated for $L_{0.5}Sr_{0.5}Co_{1-x}Ru_xO_3$ ($L$=La, Pr, Nd, Sm, and Eu) in a low-doping region of Ru ($x$=0, 0.1, and 0.2), where Ru is doped at the Co site in perovskites $L_{0.5}Sr_{0.5}CoO_3$. We recently reported the properties of $L_{0.5}Sr_{0.5}CoO_3$ ($x$=0) for $L$=Pr, Nd, Sm, and Eu (Refs. 17–19) and compared them to those of similar compounds in $L_{0.5}Ba_{0.5}CoO_{3-\delta}$.[20–23] It was found that the former compounds were metallic ferromagnets below ~230 K, while some of the latter compounds have been reported to exhibit additional antiferromagnetic order below $T_C$ and to become insulators owing to the metal-insulator transitions. Mainly from magnetic measurements, the properties of $L_{0.5}Sr_{0.5}Co_{1-x}Ru_xO_3$ were different from those of the above-mentioned manganite $Sm_{1-y}Ca_yMn_{1-x}Ru_xO_3$.

## II. EXPERIMENTAL PROCEDURES

The $L_{0.5}Sr_{0.5}Co_{1-x}Ru_xO_3$ samples ($x$=0, 0.1, and 0.2, $L$=La, Pr, Nd, Sm, and Eu) were prepared by a solid-state reaction in air; they were prepared twice to confirm the reproducibility of their properties. Stoichiometric mixtures of $L_2O_3$, $SrCO_3$, and $Co_3O_4$ and $RuO_2$ (99.9%–99.99%, Soekawa) were ground, pressed into pellets, and fired in air at 1473–1573 K for 24–48 h. The firing was repeated 2–3 times with intermediate grindings. The samples were found to contain oxygen nonstoichiometry from thermogravimetric and inductively coupled plasma (ICP) measurements. For the $x$=0.2 compounds discussed mainly below, the $\delta$ value in $L_{0.5}Sr_{0.5}CoO_{3+\delta}$ showed a tendency to decrease very slightly

 

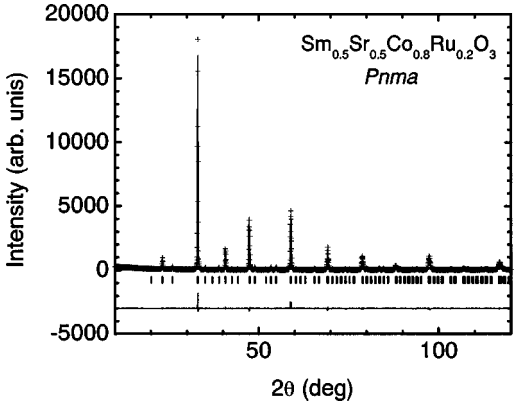


FIG. 1. XRD patterns of $Sm_{0.5}Sr_{0.5}Co_{0.8}Ru_{0.2}O_3$ (space group *Pnma*, $R_{WP}=12.38\%$, $R_P=8.67\%$, $R_e=8.32\%$, $R_I=4.13\%$, $R_F=3.97\%$). The lattice parameters are $a=5.4319(3)$ Å, $b=7.6657(3)$ Å, and $c=5.4228(2)$ Å. The cross markers and upper solid line stand for the experimental and calculated patterns, respectively. The vertical markers represent the calculated Bragg angles. The lower solid line shows the difference between the experimental and calculated intensities.

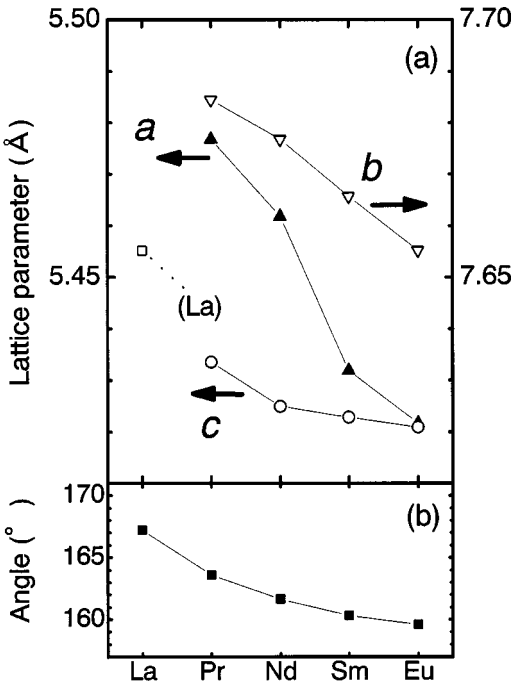


FIG. 2. (a) Lattice parameters plotted against the $L$ ion for orthorhombic $L_{0.5}Sr_{0.5}Co_{0.8}Ru_{0.2}O_3$ ($L$=Pr, Nd, Sm, and Eu). The $a$ length for rhombohedral $La_{0.5}Sr_{0.5}Co_{0.8}Ru_{0.2}O_3$ is also plotted (shown as La). (b) Averaged Co(Ru)-O-Co(Ru) angle plotted against the $L$ ion for all the $L_{0.5}Sr_{0.5}Co_{0.8}Ru_{0.2}O_3$ compounds.

from $\sim 0.04$ to $\sim -0.03$ ($\pm 0.01$–$0.02$) with increasing the atomic number of $L$. The crystal structures were determined by powder x-ray diffraction (XRD) using Cu $K\alpha$ radiation [Mac Science Co., M03XHF]. The XRD patterns were analyzed by means of the Rietveld method using the program RIETAN-2000.[25] Here dc magnetization measurements were performed in a superconducting quantum interference device (SQUID) magnetometer (Quantum Design MPMS). Magnetization-temperature ($M$-$T$) curves were measured in both field-cooled (FC) and zero-field-cooled (ZFC) modes between 4.5 and 400 K with an applied field ($H$) of 1000 Oe. Magnetization-applied field ($M$-$H$) curves were measured within $H=\pm 50\,000$ Oe at 4.5 K. Here ac magnetic susceptibilities were measured in the same apparatus. The measurement was done upon heating the sample after zero-field cooling down to 4.5 K. The field strength and frequencies of the ac field were 4 Oe and 0.8–1000 Hz, respectively. Electrical resistivity was measured by the conventional four-probe method between 4.2 and 300 K.

### III. RESULTS

Figure 1 shows the XRD patterns of $Sm_{0.5}Sr_{0.5}Co_{0.8}Ru_{0.2}O_3$. The experimental pattern could be well refined assuming a space group of orthorhombic *Pnma* with random occupation of Co and Ru at the same site. Fitting parameters such as atomic positions are comparable to those reported for other perovskites such as $SmTiO_3$.[26] The patterns of the other Ru-doped compounds could be fitted for the same *Pnma* structure except $L=$La, for which a rhombohedral $R\bar{3}c$ structure was assumed. As reported previously,[8,18] the data for the end compounds with $x=0$ ($L_{0.5}Sr_{0.5}CoO_3$) were fitted with $R\bar{3}c$, $P2_1/n$, *Pnma*, and $Pm\bar{3}m$ for $L=$La, Pr, Nd, and Sm and Eu, respectively.

All the lattice parameters increased slightly with increasing Ru content. The plausible valences of the Ru ion are 4+ or 5+.[24] From the previous studies of cobaltites,[14,18] the Co ions are likely in the LS or IS states. Though details of the change of parameters cannot be discussed here considering that the ionic radii of $Co^{3+}$ and $Co^{4+}$ were given only for the LS and HS states in the literature,[27] this result means that the average ionic radius of Co and Ru becomes larger with the Ru doping, which is reasonable because the 3*d*-metal (Co) is partially replaced by the 4*d*-metal (Ru) in the present systems. The Co(Ru)-O-Co(Ru) angles showed a tendency to decrease with the doping. This is qualitatively understood in terms of an enhancement of lattice distortion, which originates from the large average radii of the *B*-site ions (Co and Ru), as has been elucidated from many studies of perovskites. For example, the angle decreased from $\sim 166°$ to $\sim 161°$ with increasing $x$ from 0 to 0.2 for $Sm_{0.5}Sr_{0.5}Co_{1-x}Ru_xO_3$.

Figure 2(a) shows the lattice parameters for the orthorhombic $L_{0.5}Sr_{0.5}Co_{1-x}Ru_xO_3$ compounds with $x=0.2$ as well as the rhombohedral $La_{0.5}Sr_{0.5}Co_{0.8}Ru_{0.2}O_3$. The monotonic decrease in the parameters for the orthorhombic compounds is relevant to the lanthanide contraction. Figure 2(b) shows the averaged Co(Ru)-O-Co(Ru) angles plotted against the $L$ ions. The angle decreases from $\sim 167°$ ($L=$La) to $\sim 159°$ ($L=$Eu). This is attributable to the enhanced lattice distortion arising from the shrinkage of the *A*-site ion. The slight decrease in the oxygen content for the heavier $L$ ions may also be responsible for this behavior, since an averaged ionic radius of the *B*-site ions (Co and Ru) becomes larger for a lower oxidation state.

Figure 3(a) shows the $M$-$T$ curves measured with

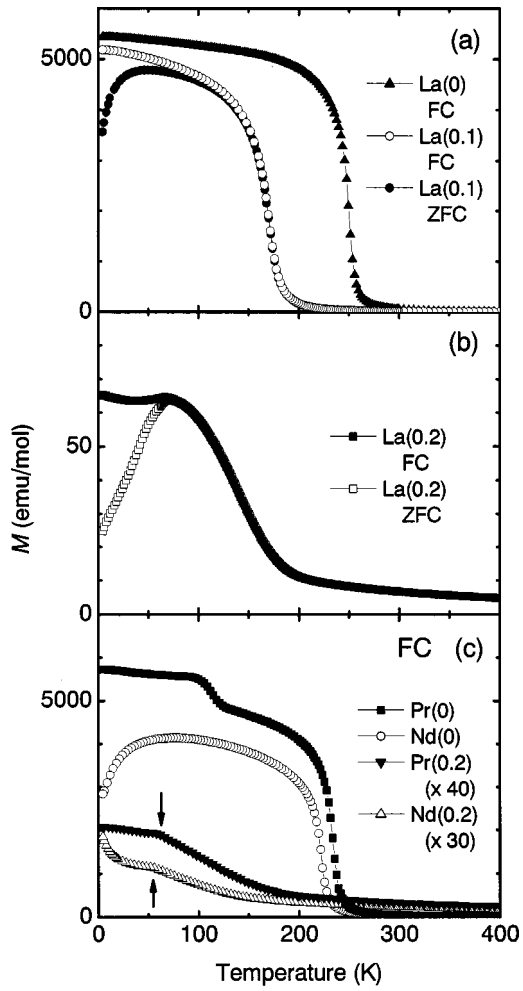


FIG. 3. *M-T* curves for (a) $La_{0.5}Sr_{0.5}Co_{1-x}Ru_xO_3$ for $x=0$ and 0.1, (b) $La_{0.5}Sr_{0.5}Co_{0.8}Ru_{0.2}O_3$ ($x=0.2$), and (c) $Pr_{0.5}Sr_{0.5}Co_{1-x}Ru_xO_3$ and $Nd_{0.5}Sr_{0.5}Co_{1-x}Ru_xO_3$. Each compound is expressed as $L(x)$, where $L$ and $x$ stand for the lanthanide and Ru content, respectively. The magnetization for $L=$Pr and Nd with $x=0.2$ was multiplied by factors of 40 and 30, respectively.

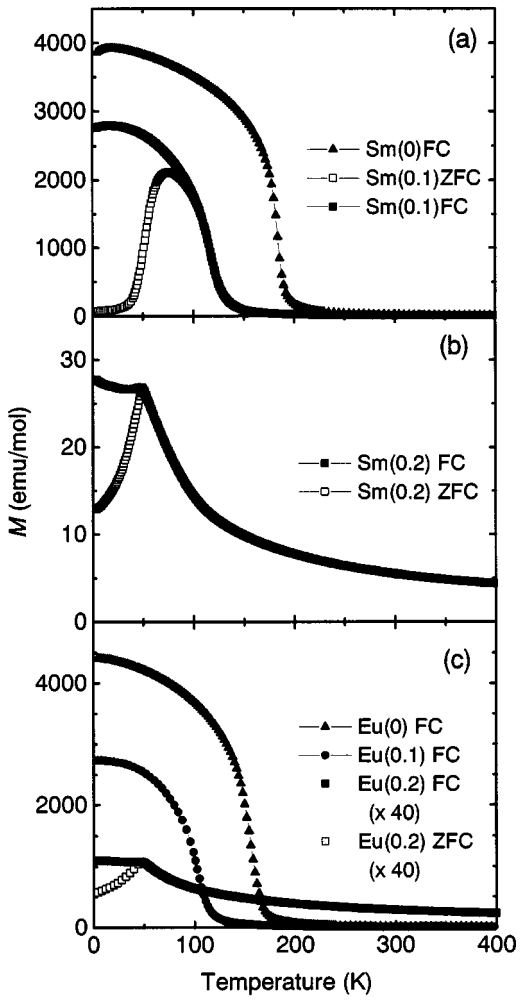


FIG. 4. *M-T* curves for (a) $Sm_{0.5}Sr_{0.5}Co_{1-x}Ru_xO_3$ with $x=0$ and 0.1, (b) $Sm_{0.5}Sr_{0.5}Co_{0.8}Ru_{0.2}O_3$ ($x=0.2$), and (c) $Eu_{0.5}Sr_{0.5}Co_{1-x}Ru_xO_3$. Each compound is expressed as $L(x)$, where $L$ and $x$ stand for the lanthanide and Ru content, respectively. The magnetization for $L=$Eu with $x=0.2$ was multiplied by a factor of 40.

$H=1000$ Oe for $La_{0.5}Sr_{0.5}Co_{1-x}Ru_xO_3$ with $x=0$ and 0.1. The ferromagnetic order takes place at $T_C\sim250$ K for $x=0$, as reported in previous papers.[3,6] From a magnetic hysteresis loop at 4.5 K, the saturation of magnetization was $\sim10^4$ emu/mol, which is close to the literature values. A high-temperature region above $T_C$ was found to obey the Curie-Weiss (CW) law. The calculated Weiss temperature was a ferromagnetic value of $\sim280$ K. The paramagnetic moment obtained from the CW fit ($\sim3.6\mu_B$) exhibited a deviation from a saturation moment ($\sim1.7\mu_B$),[3] as can be seen for itinerant magnetism.

The figure also shows that the transition temperature is lowered with a Ru doping of 10%. The transition at $\sim170$ K is brought about by the ferromagnetic order on the basis of the CW analysis, providing that there is a ferromagnetic Weiss temperature of $\sim215$ K (see Table I for brevity). The weakening of the ferromagnetic interactions is supported by the slightly smaller ordered magnetization than that for the $x=0$ compound. The deviation between the FC and ZFC curves below $\sim100$ K is in qualitative accord with the presence of magnetic transition. Figure 3(b) shows that the magnetic order is more suppressed for $x=0.2$. The ordering temperature is $\sim70$ K. The transition profiles with the absence of a steep upturn of magnetization below this temperature are antiferromagnetic rather than ferromagnetic. The FC magnetization at 4.5 K is only $\sim1/80$ as large as that of $x=0$.

The same qualitative phenomenon has also been obtained for the other systems. Figure 3(c) shows the *M-T* curves for $L=$Pr and Nd. The results for the smaller lanthanide systems of $L=$Sm and Eu are shown in Figs. 4(a)–4(c). Ferromagnetic order is observed between $\sim230$ and $\sim150$ K for the $x=0$ compounds.[18] The decrease in magnetization for $Nd_{0.5}Sr_{0.5}CoO_3$ below $\sim70$ K [Fig. 3(c)] and $Sm_{0.5}Sr_{0.5}CoO_3$ below $\sim20$ K [Fig. 4(a)] implies the evolution of ferrimagnetic coupling between the $L$ and Co moments, as found for $Nd_{0.66}Sr_{0.33}CoO_3$.[15] The ordering temperatures are lowered to $\sim50$–160 K with the doping. The transitions for $L=$Pr and Nd with $x=0.2$, exhibiting a slight inflection of magne-

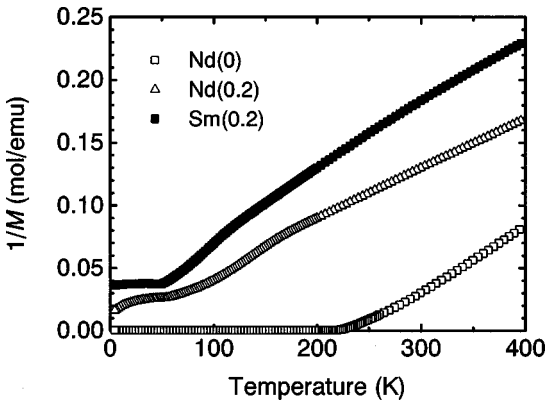


FIG. 5. Inverse magnetization plotted against temperature for $Nd_{0.5}Sr_{0.5}Co_{1-x}Ru_xO_3$ ($x=0$ and 0.2) and $Sm_{0.5}Sr_{0.5}Co_{0.8}Ru_{0.2}O_3$. Each compound is expressed as $L(x)$, where $L$ and $x$ stand for the lanthanide and Ru content, respectively.

tization at the ordering temperatures, are pointed out by the arrows in Fig. 3(c). Low-temperature magnetization is also greatly lowered by the doping in all the systems. For example, the magnetization of $Eu_{0.5}Sr_{0.5}Co_{0.8}Ru_{0.2}O_3$ is ~1/160 compared to that of $Eu_{0.5}Sr_{0.5}CoO_3$. The ZFC curves of $Sm_{0.5}Sr_{0.5}Co_{0.8}Ru_{0.2}O_3$ [Fig. 4(b)] and $Eu_{0.5}Sr_{0.5}Co_{0.8}Ru_{0.2}O_3$ [Fig. 4(c)] show sharp cusps at the transition temperature of ~50 K. This behavior is reminiscent of a spin-glass transition.[28]

Figure 5 shows inverse magnetization plotted as a function of the temperature for $Nd_{0.5}Sr_{0.5}CoO_3$, $Nd_{0.5}Sr_{0.5}Co_{0.8}Ru_{0.2}O_3$, and $Sm_{0.5}Sr_{0.5}Co_{0.8}Ru_{0.2}O_3$. The Curie-Weiss behavior is observed at high temperatures. Bending of the curvature was found at ~300 K for $Sm_{0.5}Sr_{0.5}Co_{0.8}Ru_{0.2}O_3$, which may be associated with the thermal excitation of $4f$ electrons in $Sm^{3+}$. The slope of the curve becomes slightly less steep with the doping, as speculated from the data of $Nd_{0.5}Sr_{0.5}Co_{1-x}Ru_xO_3$. This change means an increase in the effective paramagnetic moment as a result of the doping. For all $L_{0.5}Sr_{0.5}Co_{1-x}Ru_xO_3$ systems, the Weiss temperatures become smaller monotonically with increasing the Ru content, as shown later. This weakening of ferromagnetic correlation is responsible for the suppression

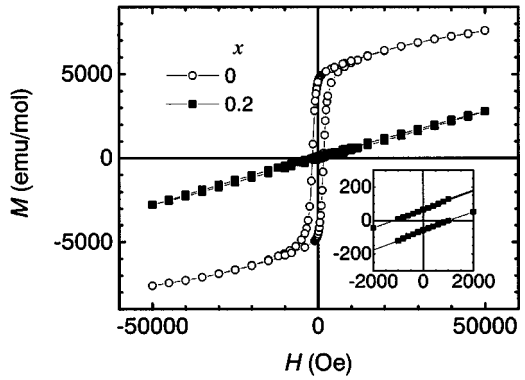


FIG. 6. *M-H* curves for $Sm_{0.5}Sr_{0.5}Co_{1-x}Ru_xO_3$ at 4.5 K for $x=0$ and 0.2. The inset shows a low-applied field region for $x=0.2$.

TABLE I. Transition temperature, effective paramagnetic moment per formula unit (including the contribution of $L$ ions), and Weiss temperature for all systems.

| | $x$ | Transition temperature (K) | Paramagnetic moment ($\mu_B$) | Weiss temperature (K) |
|---|---|---|---|---|
| La | 0 | 250 | 3.60 | 275 |
| | 0.1 | 168 | 3.32 | 215 |
| | 0.2 | 68 | 3.78 | 30 |
| Pr | 0 | 234 | 3.82 | 260 |
| | 0.1 | 159 | 3.91 | 180 |
| | 0.2 | 65 | 4.49 | −5 |
| Nd | 0 | 222 | 3.87 | 245 |
| | 0.1 | 150 | 4.03 | 165 |
| | 0.2 | 55 | 4.50 | −34 |
| Sm | 0 | 184 | 3.46 | 220 |
| | 0.1 | 117 | 3.57 | 145 |
| | 0.2 | 50 | 3.87 | −40 |
| Eu | 0 | 155 | 3.86 | 175 |
| | 0.1 | 105 | 4.06 | 115 |
| | 0.2 | 47 | 4.79 | −95 |

of magnetic order shown in Figs. 3 and 4. The change of the *M-H* curve with Ru doping, shown in Fig. 6, indicates the disappearance of magnetization saturation, which is qualitatively consistent with the behavior of the *M-T* curves.

The results obtained from the magnetization data are summarized in Table I for all compounds. The following features, including those noted above, were obtained from these figures and table. Possible origins of these phenomena will be discussed later in Sec. IV.

(1) The transition temperatures are monotonically decreased by the Ru doping in all $L_{0.5}Sr_{0.5}Co_{1-x}Ru_xO_3$ systems.

(2) Low-temperature magnetization is suppressed with the doping, which is accompanied by the disappearance of saturation magnetization.

(3) The effective paramagnetic moments tend to increase with the doping.

(4) The Weiss temperature monotonically decreases with doping. For $L_{0.5}Sr_{0.5}Co_{1-x}Ru_xO_3$ with $L=$Pr–Eu, a crossover from ferro- to antiferromagnetic interactions occurs between $x=0.1$ and 0.2.

(5) Both the transition temperature and the Weiss temperature decrease with increasing the atomic number of $L$ in $L_{0.5}Sr_{0.5}Co_{1-x}Ru_xO_3$, with $x$ having the same value.

The Ru doping also changes the electrical transport properties. Electrical resistivity ($\rho$) was plotted against the temperature ($T$) for $Sm_{0.5}Sr_{0.5}Co_{1-x}Ru_xO_3$ in Fig. 7(a). All of the $L_{0.5}Sr_{0.5}CoO_3$ ($x=0$) compounds are metallic below 300 K.[3,18] The present system shows a monotonic increase in resistivity with doping and changes to an insulator at $x=0.2$. Figure 7(b) shows the insulating nature of $La_{0.5}Sr_{0.5}Co_{1-x}Ru_xO_3$ and $Eu_{0.5}Sr_{0.5}Co_{1-x}Ru_xO_3$, exhibiting nearly identical curve shapes to those shown in Fig. 7(a). Figure 7(c) displays the plot of resistivity against $1/T$ for $Sm_{0.5}Sr_{0.5}Co_{0.8}Ru_{0.2}O_3$, which is shown as "experimental

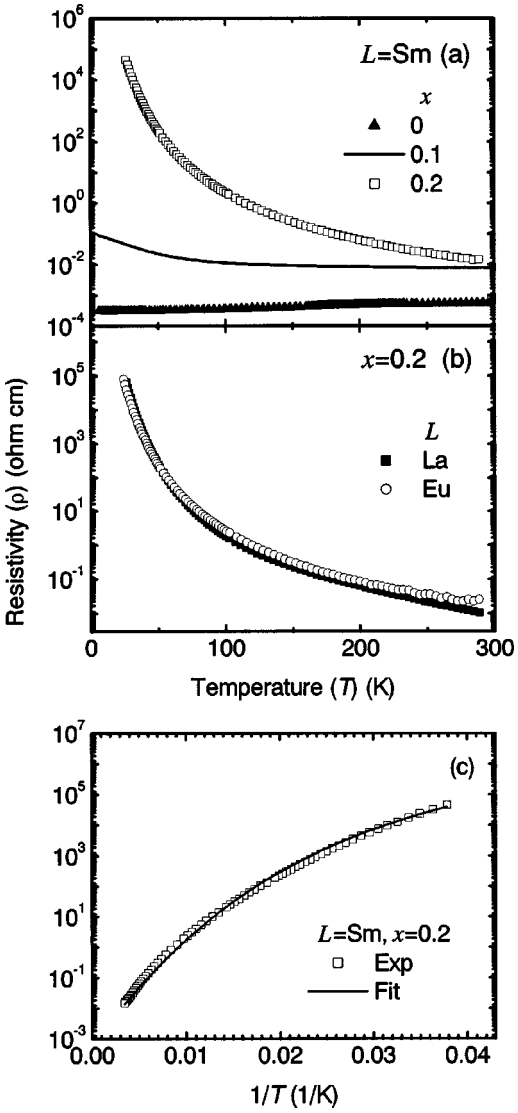


FIG. 7. Electrical resistivity ($\rho$) plotted as a function of the temperature ($T$) for (a) $Sm_{0.5}Sr_{0.5}Co_{1-x}Ru_xO_3$ and (b) $L_{0.5}Sr_{0.5}Co_{0.8}Ru_{0.2}O_3$ with $L$=La, Sm, and Eu. (c) $\rho$ values plotted against $1/T$ for $Sm_{0.5}Sr_{0.5}Co_{0.8}Ru_{0.2}O_3$. The experimental and fitted curves are shown as "Exp" and "Fit," respectively. The fit was done on the basis of the magnetically disordered model of $\rho \propto \exp[E_H/kT+(T_0/T)^{1/4}]$.

data" (Exp). The curvature shape indicates that there is no suitable fit on a simple semiconductor model of $\rho \propto \exp(E/kT)$ in the whole temperature region. The activation energies $E$ determined in the high- and low-temperature regions are shown in Table II. A successful fit at all temperatures could not be attained for other models either, such as a polaron model assumed for $LaCoO_3$ (Ref. 2) and a variable-range hopping model.[29] The parameters obtained from these models are listed in Table II. As is seen in the figure, the curve could be fitted on the magnetic polaron model for magnetically disordered systems [spin-glass polaron model, shown as "stretched exponential fit" (Fit)],[30] in which correlation effects are included in the electron-hopping processes.

TABLE II. Some parameters, such as an activation energy, calculated on the basis of the four representative models of conduction.

| Model | $E$ (meV) | $E$ (meV) |
|---|---|---|
| Semiconductor $\rho \propto \exp(E/kT)$ | 21.5 (<40 K) | 81.8 (>170 K) |
| Polaron $\rho \propto (1/T)\exp(E/kT)$ | 18.9 (<40 K) | 64.6 (>180 K) |
| | $T_0$ (K) | $T_0$ (K) |
| Variable-range hopping $\rho \propto \exp(T_0/T)^{1/4}$ | $4.50\times10^7$ (<50 K) | $2.07\times10^7$ (>140 K) |
| Magnetically disordered system $\rho \propto \exp[E_H/kT+(T_0/T)^{1/4}]$ | $E_H=82$ meV<br>$T_0=1.3\times10^7$ K | |

The fitting parameters $E_H$ and $T_0$ in $\rho \propto \exp[E_H/kT+(T_0/T)^{1/4}]$ were 82 meV and $1.3\times10^7$ K, respectively.

Figure 8 shows the real part of the ac susceptibility ($\chi'$) for $Sm_{0.5}Sr_{0.5}Co_{0.8}Ru_{0.2}O_3$. A susceptibility peak at ~50 K corresponds to the magnetic transition in the $M$-$T$ curves shown in Fig. 4(b). It shifts slightly to higher temperatures as the frequency of the ac field is increased. The result supports the speculation of a spin-glass transition. The temperature shift defined as $(\Delta T_g/T_g)(1/\Delta \log_{10}\nu)$ was calculated to be ~0.01–0.02 ($\Delta$, change of $T_g$ and $\log_{10}\nu$; $T_g$, spin-glass transition temperature; and $\nu$, frequency), assuming that $T_g$ is the peak temperature of $\chi'$. This value is comparable to those reported for typical spin glasses.[28] Almost the same shift value was also obtained for the imaginary part of the susceptibility. Much smaller shift values of ~0.002 were also obtained for the $x=0$ compounds,[19] which are comparable values to those for the Ba cobaltites $L_{0.5}Ba_{0.5}CoO_{3-\delta}$.[23] This result shows the existence of a weakly frustrated state, such as cluster glass, also in non-Ru-doped systems, originating from coexisting antiferromagnetic interactions between the Co ions.[6,14] The enhancement of the peak-temperature shift together with both the suppression of ferromagnetism and the sharp cusp, all of which are caused by the Ru doping, indicates the development of magnetic frustration originating

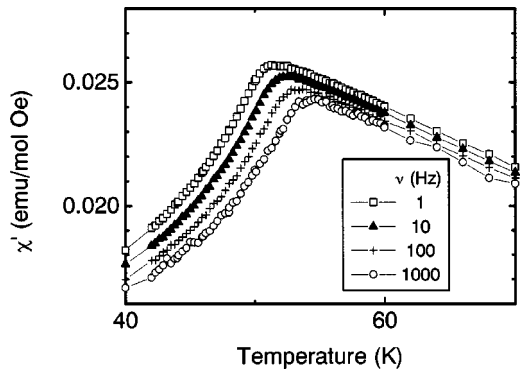


FIG. 8. Real part of the ac susceptibility for $Sm_{0.5}Sr_{0.5}Co_{0.8}Ru_{0.2}O_3$ measured with several ac frequencies ($\nu$) between 1 and 1000 Hz.

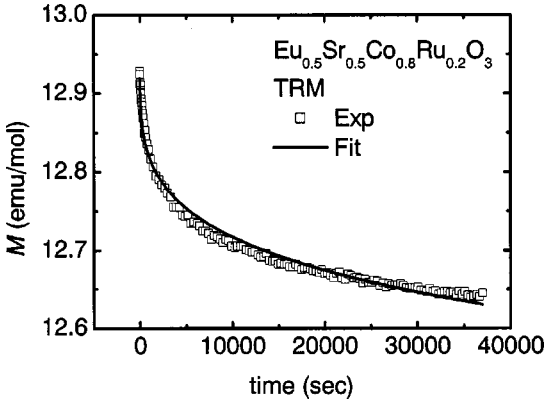


FIG. 9. Thermoremanent magnetization (TRM) plotted against time for $Eu_{0.5}Sr_{0.5}Co_{0.8}Ru_{0.2}O_3$ measured at 6 K. The experimental data and stretched exponential fit are shown as ''Exp'' and ''Fit,'' respectively.

from the strengthened antiferromagnetic interactions. Figure 9 presents the temperature dependence of thermoremanent magnetization (TRM) measured for $Eu_{0.5}Sr_{0.5}Co_{0.8}Ru_{0.2}O_3$. The sample was cooled from room temperature to 5 K in an applied field of 1000 Oe. The measurement was done immediately after reducing the field to zero. The relaxation of magnetization could be fitted with a stretched exponential form $M_0 \exp(-\alpha t^n)$ ($M_0$, initial magnetization; $t$, time) for some glassy compounds.[31,32] The $\alpha$ and $n$ values were estimated to be $\sim 0.0022$ and $\sim 0.24$, respectively, both of which could change from system to system depending on some physical parameters as well, such as the measurement temperature.[31,32]

## IV. DISCUSSION: POSSIBLE ORIGINS OF MAGNETIC BEHAVIOR

The metallic ferromagnetism in the Ru-free $L_{0.5}Sr_{0.5}CoO_3$ ($x=0$) is interpreted likely on the basis of the discussion for $La_{1-x}Sr_xCoO_3$, in which a ferromagnetic interaction between $Co^{3+}$ and $Co^{4+}$ arises from the averaged intermediate spin state of $t_{2g}^5 e_g^{(1-x)}$.[1,3] From isothermal magnetization measurements at 4.5 K, this spin state is plausible also for $L_{0.5}Sr_{0.5}CoO_3$ with $L=$Pr–Eu, implying the coexistence of IS $Co^{3+}$ ($t_{2g}^5 e_g^1$) and LS $Co^{4+}$ ($t_{2g}^5 e_g^0$).[18] For the analogous system $L_{0.66}Sr_{0.33}CoO_3$ ($L=$La, Pr, $Pr_{0.5}Nd_{0.5}$, Nd, $Nd_{0.5}Sm_{0.5}$, and Sm), the presence of IS $Co^{3+}$ ($t_{2g}^5 e_g^1$), LS $Co^{4+}$ ($t_{2g}^5 e_g^0$), and IS $Co^{4+}$ ($t_{2g}^4 e_g^1$) was suggested.[14]

The expansion of ferromagnetism and metallicity in the manganite $Sm_{1-y}Ca_yMn_{1-x}Ru_xO_3$ (Ref. 24) is in contrast with the present results and is somewhat unexpected because similar mechanisms are assumed for the ferromagnetism in both $L_xA_xMnO_3$ and $L_{1-x}A_xCoO_3$. One possible reason for the behavior in $Sm_{1-y}Ca_yMn_{1-x}Ru_xO_3$ is that the Mn ions remain in the $Mn^{3+}$ ($t_{2g}^3 e_g^1$) and $Mn^{4+}$ ($t_{2g}^3 e_g^0$) states, which have ferromagnetic interactions with the low-spin ions of $Ru^{4+}$ ($t_{2g}^4 e_g^0$) or $Ru^{5+}$ ($t_{2g}^3 e_g^0$) via an electron transfer between the $e_g$ orbitals.

On the other hand, all the present $L_{0.5}Sr_{0.5}Co_{1-x}Ru_xO_3$ systems show the evolution of antiferromagnetic correlation by the Ru doping. It is plausible that the Ru ions are stabilized in the low-spin state for both $Ru^{4+}$ and $Ru^{5+}$, as suggested by the experimental results of perovskite ruthenates such as $CaRuO_3$ and $SrRuO_3$.[33–35] A valence fluctuation between $Ru^{4+}$ and $Ru^{5+}$ is likely to occur as well. Different from the case of the $L_{0.5}Sr_{0.5}CoO_3$ ($x=0$) metallic compounds, paramagnetic moments obtained from the Curie-Weiss analysis for the Ru-doped $x=0.2$ compounds reflect actual spin states because of their localized nature, as is revealed from the resistivity measurements (Fig. 7). The calculated paramagnetic moments for the two ionic states of Ru, together with the spin states of Ru and Co, are listed in Table III for $Nd_{0.5}Sr_{0.5}Co_{0.8}Ru_{0.2}O_3$, which was selected as a representative system considering the ambiguity of the Sm and Eu systems due to the thermal excitation of $4f$ electrons. The effective $Nd^{3+}$ moment of $3.68\mu_B$ was used in the calculation.[36] From the experimental work on $L_{0.66}Sr_{0.33}CoO_3$ (Ref. 14) and $L_{0.5}Sr_{0.5}CoO_3$ (Ref. 18), it seems to be plausible that the $Co^{3+}$ and $Co^{4+}$ ions are in the LS and/or IS state. However, Tables I and III show that each

TABLE III. Upper panel: valence of Ru, average valence of Co, some representative electronic states of Co, and calculated paramagnetic moment including the contribution of $Nd^{3+}$ for $Nd_{0.5}Sr_{0.5}Co_{0.8}Ru_{0.2}O_3$. Lower panel: Electronic states of the spin states of Co and Ru ions and spin-only magnetic moments, which were used for the calculation of the values in the upper panel.

| $Ru^{4+}$ $Co^{3.375+}$ | Electronic state of Co | Estimated paramagnetic moment ($\mu_B$) |
|---|---|---|
| | $Co^{3+}$+(LS)$Co^{4+}$(LS) | 3.04 |
| | $Co^{3+}$(IS)$Co^{4+}$(LS) | 3.64 |
| | $Co^{3+}$(IS)$Co^{4+}$(IS) | 4.11 |
| | $Co^{3+}$(HS)$Co^{4+}$(IS) | 4.99 |
| | $Co^{3+}$(IS)$Co^{4+}$(HS) | 4.78 |
| $Ru^{5+}$ $Co^{3.125+}$ | Electronic state of Co | Estimated paramagnetic moment ($\mu_B$) |
| | $Co^{3+}$+(LS)$Co^{4+}$(LS) | 3.17 |
| | $Co^{3+}$(IS)$Co^{4+}$(LS) | 3.96 |
| | $Co^{3+}$(IS)$Co^{4+}$(IS) | 4.11 |
| | $Co^{3+}$(HS)$Co^{4+}$(IS) | 5.30 |
| | $Co^{3+}$(IS)$Co^{4+}$(HS) | 4.34 |
| | Electronic states | Spin-only moment ($\mu_B$) |
| $Co^{3+}$ | LS($t_{2g}^6 e_g^0$) | 0 |
| | IS($t_{2g}^5 e_g^1$) | 2.83 |
| | HS($t_{2g}^4 e_g^2$) | 4.90 |
| $Co^{4+}$ | LS($t_{2g}^5 e_g^0$) | 1.73 |
| | IS($t_{2g}^4 e_g^1$) | 3.87 |
| | HS($t_{2g}^3 e_g^2$) | 5.92 |
| $Ru^{4+}$ | LS($t_{2g}^4 e_g^0$) | 2.83 |
| $Ru^{5+}$ | LS($t_{2g}^3 e_g^0$) | 3.87 |

calculated moment on this assumption is smaller than the experimental value, even in the case for the IS state for both $Co^{3+}$ and $Co^{4+}$, which provide the largest paramagnetic moments. This result was true also for the other $x=0.2$ compounds from the calculation using the effective $L^{3+}$ moments in Ref. 36. If the oxygen nonstoichiometry is taken into account, the average valences of Co are $\sim$3.3–3.5+ and $\sim$3.0–3.3+ for the $Ru^{4+}$ and $Ru^{5+}$ substitutions, respectively. These values give the same qualitative result from the same type of calculation. The analyses described here strongly suggests that the Co ions are partially converted into the HS state and have larger spin-only moments, though the contents of the spin states of the Co ions cannot be determined from the magnetization data alone.The larger radius of the HS ion than that of the LS ion calculated for $Co^{3+}$ (Ref. 27) is consistent with the enhancement of the lattice distortion noted in Sec. III.

The crystallographic change is not responsible for the conversion of the spin state. As was noted, the Ru doping makes the Co(Ru)-O-Co(Ru) angle smaller for each system. This change reduces energy widths of the $t_{2g}$–$e_g$ bands due to a decrease in electron transfer. Thus the energy gap between the $t_{2g}$ and $e_g$ bands is increased, which suppresses the electron excitation from $t_{2g}$ to $e_g$. Widening of the energy gap was suggested from the optical study on the perovskites, including the cobaltites $LaCoO_3$ and $YCoO_3$, where the latter compound has a larger lattice distortion.[37]

The spin-state conversion is interpreted in connection with the stronger covalency of Ru 4*d* orbitals than of Co 3*d*, as was commented previously.[24] The Ru doping broadens the energy widths of both the $t_{2g}$ and $e_g$ bands and consequently leads to a narrowing of the energy gap. Therefore, electron excitation from $t_{2g}$ to $e_g$, which leads to the HS state, is promoted. The presence of the HS state explains the weakening of ferromagnetic interactions revealed from the Curie-Weiss analysis (Table I), since electron transfers between the $e_g$ orbitals of the HS Co ions dominantly generate antiferromagnetic interactions. As a result of magnetic frustration intensified by the strengthened antiferromagnetic correlation, the transition temperature and the ordered magnetization become lower (Table I). For the manganite $Sm_{1-y}Ca_yMn_{1-x}Ru_xO_3$, a wider energy difference between the $t_{2g}$ and $e_g$ states is assumed. This situation may be related to the smaller optical gap in the perovskite $LaCoO_3$ than in $LaMnO_3$.[37]

The insulating behavior caused by the doping (Fig. 7) means that the on-site Coulomb energy ($U$) at Co overcomes the energy width of the $e_g$ band ($W$).[4] In other words, this band is not wide enough to contain the three or four electrons that are required for electrical conductivity. The insulating nature of the present compounds, different from the metallicity of $Sm_{1-y}Ca_yMn_{1-x}Ru_xO_3$, can be understood in terms of a larger $U$ value per 3*d* electron in the Co ions than in the Mn ions, owing to the larger number of 3*d* electrons in the former ions. In spite of very slight differences in the $U$ values, this tendency is found from the theoretical calculation for some compounds.[38] The fit for the experimental data on the magnetically disordered model [Fig. 7(c)] indicates that correlation effects and disorder play a significant role in the conduction process, which is in accordance with the presence of magnetic frustration.

The antiferromagnetic interaction for each of the $x=0.1$ and $x=0.2$ series also became stronger for the heavier $L$ ions (Table I). The magnetic frustration is the largest for $Eu_{0.5}Sr_{0.5}Co_{0.8}Ru_{0.2}O_3$, which shows the lowest transition temperatures of 47 K accompanied by the spin-glass behavior. The tendency is likely associated with weaker ferromagnetic $Co^{3+}$-$Co^{4+}$ couplings, owing to the narrowing of the Co(Ru)-O-Co(Ru) angle for the heavier $L$ ions [Fig. 2(b)], as suggested for the monotonic decrease in $T_C$ for $L_{0.66}Sr_{0.33}CoO_3$ with increasing the atomic number of $L$.[14] However, as such narrowing also lowers the antiferromagnetic interactions between Co and Ru, the tendency could not be understood only in this context alone. Theoretical investigations for estimating the strengths of ferro- and antiferromagnetic interactions are necessary. Another possibility for the enhancement of the antiferromagnetic correlation is the tendency of a slight decrease in $\delta$ for $L_{0.5}Sr_{0.5}Co_{0.8}Ru_{0.2}O_{3+\delta}$ as the atomic number of $L$ is increased (Sec. II); however, it should be noted that the change of $\delta$ is very slight and is comparable to the experimental errors. As it is plausible that such a change lowers the content of $Co^{4+}$ because of the reduction of Co and Ru, the ferromagnetic coupling between $Co^{3+}$ and $Co^{4+}$ is further weakened for the heavier lanthanides. A similar explanation is also applicable to the metallic $L_{0.5}Sr_{0.5}CoO_{3+\delta}$ ($x=0$) compounds, which show a monotonic decrease in both $T_C$ and $\delta$ with increasing the atomic number of $L$ (Refs. 18 and 39) and in which no clear relationship between $T_C$ and the Co-O-Co angle is observed.

## V. SUMMARY

Structure, magnetism, and transport have been investigated for $L_{0.5}Sr_{0.5}Co_{1-x}Ru_xO_3$ ($L$=La, Pr, Nd, Sm, and Eu, $x=0$, 0.1, and 0.2), where Ru is doped at the Co site in perovskite cobaltites $L_{0.5}Sr_{0.5}CoO_3$. The structures of most of the compounds were refined to orthorhombic *Pnma*. The compounds $L_{0.5}Sr_{0.5}CoO_3$ ($x=0$) are metallic ferromagnets below Curie temperatures between $\sim$250 and $\sim$150 K. It was found that Ru doping brings about the suppression of the ferromagnetic order as well as the loss of metallicity. The Curie-Weiss analysis showed that the order (except for $L$=La) commonly changed into that of the antiferromagnetic type with the doping. For $L$=Sm and Eu with $x=0.2$, sharp cusps at around 50–60 K in the magnetization-temperature curves were ascribed to a spin-glass transition, a finding which was supported by measurements of ac magnetic susceptibility and magnetization relaxation. An origin of these phenomena is proposed by considering several factors such as the change of the spin states of Co induced by Ru doping.

*Note added in proof.* The crystal structure of one of the $x=0$ compounds, $Eu_{0.5}Sr_{0.5}CoO_3$ was reported recently to be monoclinic $P2_1/m$ (No. 11).[40] As a crystallographic distortion is expected to be larger for heavier lanthanide

ions, this result seems to be relevant, as noted by the authors of this paper. This structure for our samples led to lattice lengths [$a=5.3721(11)$, $b=7.5947(6)$, and $c=5.3718(10)$ Å, $\beta=89.713(8)°$, $R_{WP}\sim 11\%$, goodness-of-fit $\sim 1.4$] which are close to those in this paper. For this structure, no apparent relationship between the Curie temperature and the Co-O-Co angle was observed for the $x=0$ series $L_{0.5}Sr_{0.5}CoO_3$. Higher resolution measurements, such as synchrotron x-ray diffraction, are required to obtain further information.

*Corresponding author. FAX: +81-791-58-2740. Electronic address: yoshiike@spring8.or.jp

[1] R. Caciuffo, D. Rinaldi, G. Barucca, J. Mira, J. Rivas, M. A. Señarís-Rodríguez, P. G. Radaelli, D. Fiorani, and J. B. Goodenough, Phys. Rev. B **59**, 1068 (1999), and references therein.
[2] M. A. Señarís-Rodríguez and J. B. Goodenough, J. Solid State Chem. **116**, 224 (1995).
[3] M. A. Señarís-Rodríguez and J. B. Goodenough, J. Solid State Chem. **118**, 323 (1995).
[4] J. B. Goodenough, J. Alloys Compd. **262**, 1 (1997).
[5] M. R. Ibarra, R. Mahendiran, C. Marquina, B. García-Landa, and J. Blasco, Phys. Rev. B **57**, R3217 (1998).
[6] M. Itoh, I. Natori, S. Kubota, and K. Motoya, J. Phys. Soc. Jpn. **63**, 1486 (1994).
[7] P. S. Anil Kumar, P. A. Joy, and S. K. Date, J. Phys.: Condens. Matter **10**, L487 (1998).
[8] A. Mineshige, M. Inaba, T. Yao, Z. Ogumi, K. Kikuchi, and M. Kawase, J. Solid State Chem. **121**, 423 (1996).
[9] A. Barman, M. Ghosh, S. K. De, and S. Chatterjee, Phys. Lett. A **234**, 384 (1997).
[10] C. N. R. Rao, O. M. Parkash, D. Bahadur, P. Ganguly, and S. Nagabhushana, J. Solid State Chem. **22**, 353 (1977).
[11] G. Ch. Kostogloudis, N. Vasilakos, and Ch. Ftikos, Solid State Ionics **106**, 207 (1998).
[12] H. W. Brinks, H. Fjellvåg, A. Kjekshus, and B. C. Hauback, J. Solid State Chem. **147**, 464 (1999).
[13] M. A. Señarís-Rodríguez, M. P. Breijo, S. Castro, C. Rey, M. Sánchez, R. D. Sánchez, J. Mira, A. Fondado, and J. Rivas, Int. J. Inorg. Mater. **1**, 281 (1999).
[14] M. Paraskevopoulos, J. Hemberger, A. Krimmel, and A. Loidl, Phys. Rev. B **63**, 224416 (2001).
[15] A. Krimmel, M. Reehuis, M. Paraskevopoulos, J. Hemberger, and A. Loidl, Phys. Rev. B **64**, 224404 (2001).
[16] R. Ganguly, M. Hervieu, N. Nguyen, A. Maignan, C. Martin, and B. Raveau, J. Phys.: Condens. Matter **13**, 10911 (2001).
[17] K. Yoshii and A. Nakamura, Physica B **281-282**, 514 (2000).
[18] K. Yoshii, H. Abe, and A. Nakamura, Mater. Res. Bull. **36**, 1447 (2001).
[19] K. Yoshii, A. Nakamura, H. Abe, M. Mizumaki, and T. Muro, J. Magn. Magn. Mater. **239**, 85 (2002).
[20] I. O. Troyanchuk, N. V. Kasper, D. D. Khalyavin, H. Szymczak, R. Szymczak, and M. Baran, Phys. Rev. B **58**, 2418 (1998).
[21] Y. Moritomo, M. Takeo, X. J. Liu, T. Akimoto, and A. Nakamura, Phys. Rev. B **58**, R13 334 (1998).
[22] Y. Moritomo, T. Akimoto, M. Takeo, A. Machida, E. Nishibori, M. Takata, M. Sakata, K. Ohoyama, and A. Nakamura, Phys. Rev. B **61**, R13 325 (2000).
[23] A. Maignan, C. Martin, D. Pelloquin, N. Nguyen, and B. Raveau, J. Solid State Chem. **142**, 247 (1999).
[24] C. Martin, A. Maignan, M. Hervieu, C. Autret, B. Raveau, and D. I. Khomskii, Phys. Rev. B **63**, 174402 (2001), and references therein.
[25] F. Izumi and T. Ikeda, Mater. Sci. Forum **321–324**, 198 (2000).
[26] For example, G. Amow, J. E. Greedan, and C. Ritter, J. Solid State Chem. **141**, 262 (1998).
[27] R. D. Shannon, Acta Crystallogr., Sect. A: Cryst. Phys., Diffr., Theor. Gen. Crystallogr. **32**, 751 (1976).
[28] J. A. Mydosh, *Spin Glasses* (Taylor & Francis, London, 1993).
[29] N. F. Mott and E. A. Davis, *Electronic Process in Non-Crystalline Materials*, 2nd ed., (Clarendon, Oxford, 1979).
[30] A. S. Ioselevich, Phys. Rev. Lett. **71**, 1067 (1993).
[31] G. C. DeFotis, G. S. Coker, J. W. Jones, C. S. Branch, H. A. King, J. S. Bergman, S. Lee, and J. R. Goodey, Phys. Rev. B **58**, 12 178 (1998).
[32] K. Yamaura, Q. Huang, and R. J. Cava, J. Solid State Chem. **146**, 277 (1999).
[33] H. Mukuda, K. Ishida, Y. Kitaoka, K. Asayama, R. Kanno, and M. Takano, Phys. Rev. B **60**, 12 279 (1999).
[34] I. Felner, I. Nowik, I. Bradaric, and M. Gospodinov, Phys. Rev. B **62**, 11 332 (2000).
[35] T. He and R. J. Cava, Phys. Rev. B **63**, 172403 (2001).
[36] J. H. Van Vleck, *The Theory of Electric and Magnetic Susceptibilities* (Oxford University Press, New York, 1965).
[37] T. Arima, Y. Tokura, and J. B. Torrance, Phys. Rev. B **48**, 17 006 (1993).
[38] J. B. Torrance, P. Lacorre, C. Asavaroengchai, and R. M. Metzger, Physica C **182**, 351 (1991).
[39] K. Yoshii *et al.* (unpublished).
[40] R. Ganguly *et al.*, J. Phys.: Condens. Matter **14**, 8595 (2002).